Catalysis Letters
https://doi.org/10.1007/s10562-020-03172-5

Synthesis of a Cellulosic Pd(salen)-Type Catalytic Complex as a Green and Recyclable Catalyst for Cross-Coupling Reactions

Peng Sun[1,2] · Jiaojiao Yang[1] · Chunxia Chen[1,2] · Kaijun Xie[1] · Jinsong Peng[1]

Received: 25 November 2019 / Accepted: 8 March 2020

Abstract

A green recyclable cellulose-supported Pd(salen)-type catalyst was synthesized through sequential three steps: chlorination with thionyl chloride, modification by ethylenediamine, and the formation of Schiff base with salicylaldehyde to immobilize palladium chloride through multiple binding sites. This novel heterogeneous cellulosic Pd(salen)-type catalytic complex was fully characterized by FT-IR, SEM, TEM, XPS, ICP-AES and TG. The traditional cross-coupling chemistry, such as Suzuki, Heck, Sonogashira, Buchwald–Hartwig amination and etherification, was then investigated in the presence of the above cellulose-palladium nanoparticle. Studies have shown that the synthesized catalyst shows high activity and efficiency for all types of transformations, providing the corresponding carbon–carbon or carbon–heteroatom coupling products in a general and mild manner. Furthermore, the catalyst demonstrates high to excellent yields and is easily recycled by simple filtration for up to twelve cycles without any significant loss of catalytic activity.

Graphic Abstract

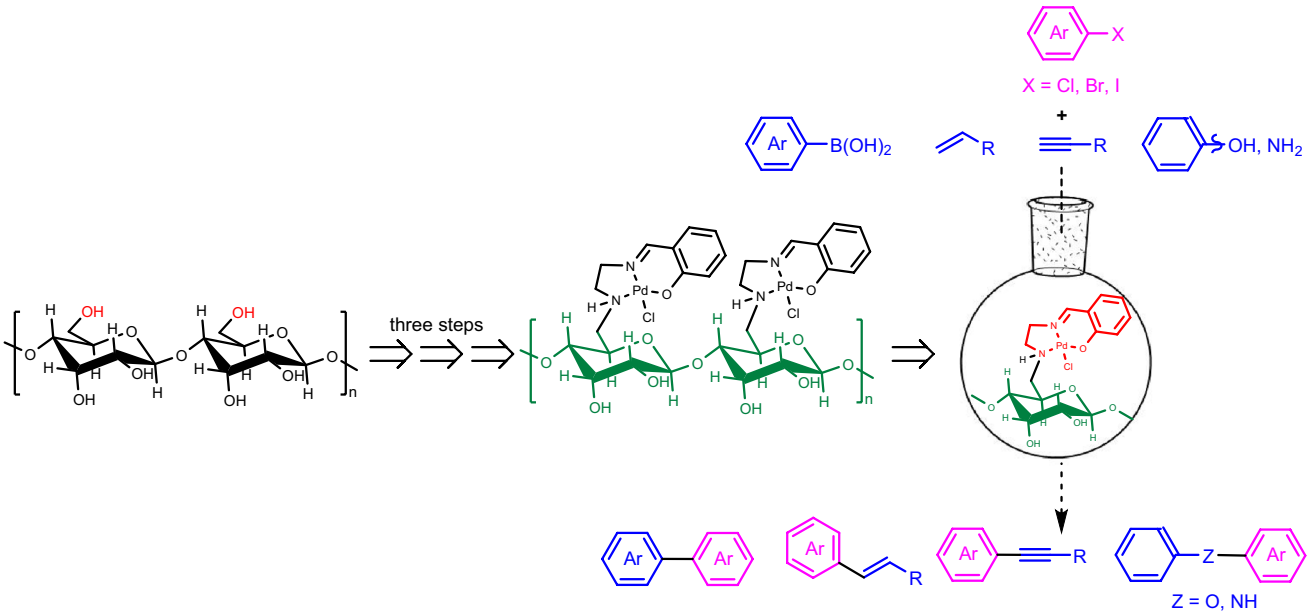

Keywords Cellulose · Salen-type ligand · Pd catalysis · Heterogeneous · Cross-coupling reactions

Electronic Supplementary Material The online version of this article (https://doi.org/10.1007/s10562-020-03172-5) contains supplementary material, which is available to authorized users.

Extended author information available on the last page of the article

Published online: 28 March 2020

1 Introduction

Pd-catalyzed cross-coupling reactions, such as Suzuki–Miyaura, Heck, Sonogashira, Buchwald–Hartwig amination and etherification, have emerged as powerful tools for carbon–carbon and carbon–heteroatom bond formation in synthetic organic chemistry [1, 2], displaying broad applications in the preparation of materials, natural products and biologically active compounds [3, 4]. Generally, these coupling reactions are carried out in the presence of a homogeneous palladium catalyst. However, the high costs associated with palladium and ligands, the difficulties in product separation and recycling of the catalyst, and the lack of generality toward all types of cross-coupling reactions obviously do not meet the prospects of contemporary green and sustainable chemistry development [5, 6]. To overcome these disadvantages, researchers have turned to the design and development of palladium complexes with broader activity immobilized on environmentally benign supports. Over the past decades, various solid materials, such as polymers [7, 8], activated carbon [9], clays [10], and magnetic nanoparticles (MNPs) [11] have been performed.

Recently, as people attach great importance to the increasingly severe ecological environment, the replacement of petrochemical-based materials with biodegradable materials has attracted more and more research priorities. A variety of biodegradable polysaccharides such as chitosan [12–17], agar [18, 19] and starch [20] supported heterogeneous catalysts for organic synthetic chemistry came into being. Compared with other carbon sources, microcrystalline cellulose has a higher specific surface area, high thermal and chemical stability, and is one of the most abundant, renewable and ecofriendly nature carbon precursors in the world [21–24]. Thus, a series of cellulose-supported metal nanoparticles such as Ag [25, 26], Al [27], Au [28, 29], Cr [30], Cu [31, 32], Pd [33, 34], Pt [35] Rh [36] were developed. Among these, palladium nanoparticles have garnered maximum attention due to their versatile catalytic activity for many organic reactions including cross-coupling [37], hydrogenation [38], cyclization [39] and oxidation [40].

As early as 2006, Reddy prepared a cellulose supported Pd(0) catalyst for Heck and Sonogashira reactions with aryl iodides as substrates [41]. However, since Pd was bound to cellulose only by adsorption, the catalytic activity was significantly decreased due to leaching and aggregation of Pd(0) after 4 cycles. Therefore, the strategy through ligand-anchored cellulose to coordinate with palladium was rapidly developed to solve problems like catalyst deactivation and metal leaching [42]. In 2012, Li carried out diphenylphosphinite cellulose-supported nano-palladim catalyst for Heck reaction in a mild condition [43]. After this, a lot of similar studies were reported [44, 45]. However, due to the toxicities of traditional phosphine ligands, air sensitivity and high cost, which will limit the application in the field of catalysis. Schiff bases have been used as powerful and useful ligands for promoting transition metal-based catalysis [46, 47]. In addition, Schiff bases have advantages over free phosphine ligands, *N*-heterocyclic carbene, and amines ligands because of their superior electronic properties, different oxidation states, non-toxicity, and ease of preparation, which are particularly significant for retaining metal species and meeting the demand of sustainable chemistry [48–50].

Herein, we designed and prepared a new, efficient and recyclable heterogeneous palladium catalyst based on functionalized cellulose as a biopolymers support. At first, microcrystalline cellulose is chlorinated by thionyl chloride, then modified using ethylenediamine, and finally reacted with simple and affordable salicylaldehyde to form Cell-Schiff base. Afterwards, Cell-Schiff base was added to a $PdCl_2$ solution to obtain the cellulosic Pd(salen)-type catalyst (Scheme 1). The prepared catalyst is characterized by FT-IR, SEM, TEM, XPS, ICP-AES and TG techniques and was then used for cross-coupling reactions of between haloarenes and different nucleophilic partners to obtain coupling products.

2 Materials and Methods

2.1 Materials and Instrumentation

All chemicals were used as received unless otherwise stated. Microcrystalline cellulose, thionyl chloride, ethylenediamine, salicylaldehyde, palladium chloride ($PdCl_2$), aryl boronic acid, aryl halides, aryl acetylene, styrene, aniline, and phenol were purchased from Shanghai Energy Co. Ltd, China. All other reagents and solvents such as *N,N*-dimethylformamide (DMF), dimethyl sulfoxide (DMSO), ethyl alcohol, acetone, potassium carbonate, ethyl acetate (EA), and $MgSO_4$ were purchased from Tianjin Fuyu Chemical Co. Ltd, China.

The Fourier Transform Infrared Spectrometer (FT-IR) spectra of the samples were obtained by a Perkin Elmer Spectrum 100 FT-IR spectrophotometer. Scanning Electron Microscope (SEM) images of all products were taken on a JSM-7500F. Transmission Electron Microscope (TEM) image of the catalyst was performed on a JEM-2100*operated at an accelerating voltage of 200 kV. X-ray photoelectron spectroscopy (XPS) was measured on X, Pert3 Powedr (at 52 kV, 60 mA, 3 kW). X-Ray diffraction spectrum (XRD) was recorded on XRD-6100 Produced by Shimadzu Corporation of Japan (at 60 kV, 80 mA, and 2θ with

Scheme 1 Synthetic route of the cellulosic Pd(salen)-type catalyst

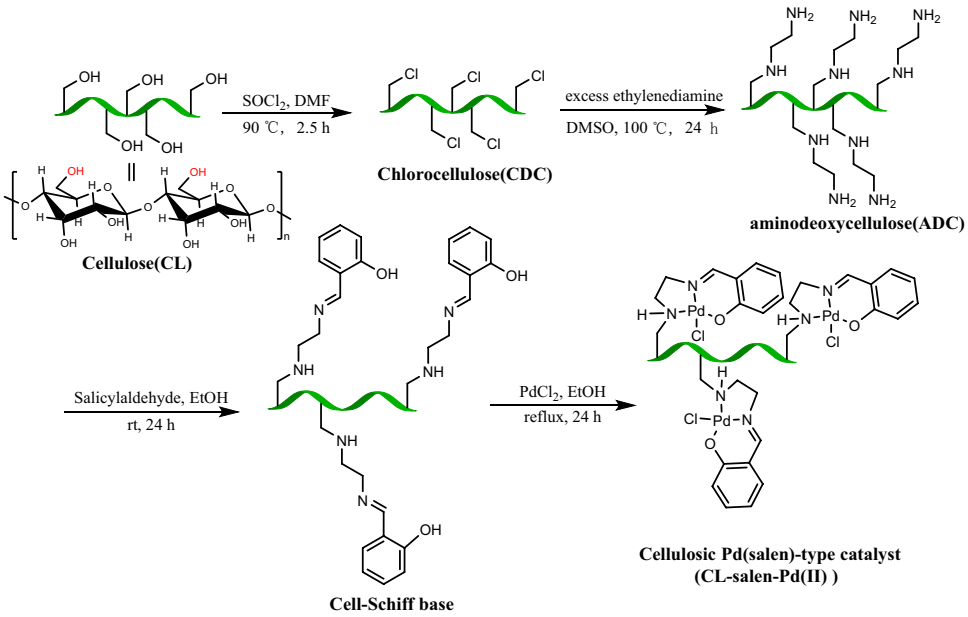

a scan angle: 5°–80°). The palladium content of the catalyst was investigated with a Spectro Blue Inductively coupled plasma mass spectrometry (ICP-AES). Thermal stability of materials was measured on a STA449F3 from room temperature to 800 ℃. The ^{1}H NMR spectra were performed on a 500 MHz Bruker Ultrashield instrument with Chloroform-d solvents and tetramethylsilane internal standard. TLC analysis (20 cm × 20 cm) was conducted on Silica Gel 60 F254.

2.2 Modification of Cellulose

Microcrystalline cellulose (30.8 mmol, 5 g) and DMF (100 mL) were added to a four-necked bottle equipped with a stirrer, a drying tube and an exhaust gas absorption device. $SOCl_2$ (30.8 mmol, 16.4 mL) was slowly added under stirring at 80 ℃, then the mixture was reacted for 2.5 h at 90 ℃. After cooling to room temperature, the mixture was poured into 500 mL of cold water. The precipitate was filtered and washed with distilled water to neutral, the obtained chlorocellulose (CDC) was then dried overnight at 50 ℃ under vacuum. Subsequently, excess ethylenediamine was added to a mixture of dried CDC in DMSO and then stirred at 100 ℃ for 24 h, the reaction was terminated by adding distilled water, and the precipitate was filtered and washed with acetone until colorless. The product aminodeoxycellulose (ADC) was dried overnight at 50 ℃ under vacuum (Scheme 1).

2.3 Preparation of the Catalyst

Salicylaldehyde (4.76 mmol, 1.12 g) was added to a suspension of ADC (4.76 mmol, 1.12 g) in anhydrous ethanol and stirred at room temperature for 2 h. The Cell-Schiff base was dried overnight at 50 °C under vacuum after filtration and washing with ethanol. Subsequently, $PdCl_2$ (5.23 mmol, 195.06 mg) was added to a suspension of the dried Cell-Schiff base in ethanol, and the mixture was stirred at 80 °C to for 24 h form cellulosic Pd(salen)-type catalyst (CL-salen-Pd(II)). Finally, the catalyst was filtrated and washed by ethanol, and dried overnight at 50 °C under vacuum (Scheme 1).

2.4 General Procedure for Palladium-Catalyzed Cross Coupling Reactions

2.4.1 Suzuki Cross-Coupling Reaction

A flame-dried 50 mL round-bottom flask equipped with a magnetic stir bar and a rubber septum was charged with aryl halide (1.0 mmol), phenyl boronic acid (1.1 mmol), K_2CO_3 (2.0 mmol) and CL-salen-Pd(II) (0.5% mmol). The mixture was stirred in Ethanol: H_2O = 1:1 (5.0 mL) at 50 ℃ under air atmosphere for 1 h. The mixture was cooled to room temperature, quenched with water (5 mL), and diluted with ethyl acetate (5 mL). The layers were separated, and the aqueous layer was extracted with 2 × 5 mL of ethyl acetate. The combined organic extracts were dried over anhydrous magnesium sulfate, filtered, and concentrated in vacuo. Finally, the product was purified by column chromatography.

2.4.2 Heck Reaction

A flame-dried 50 mL round-bottom flask equipped with a magnetic stirbar and a rubber septum were charged with aryl halide (1.0 mmol), alkene substrate (1.1 mmol), K_2CO_3 (2.0 mmol) and CL-salen-Pd(II) (1.0% mmol). Then ethanol

(5.0 mL) was added and the mixture was heated to reflux under air atmosphere for 3 h. After that, the mixture was cooled to room temperature, filtered, washed with diethyl ether, and concentrated in vacuo. The residue was finally purified by column chromatography.

2.4.3 Sonogashira Cross-Coupling Reaction

A flame-dried 50 mL round-bottom flask equipped with a magnetic stirbar and a rubber septum were charged with aryl halide (1.0 mmol), terminal alkyne (1.1 mmol), CuI (0.05 mmol), K_2CO_3 (2.0 mmol) and CL-salen-Pd(II) (1.0% mmol). Ethanol (5.0 mL) was then added and the mixture was heated to reflux under air atmosphere for 3 h. After extraction with ethyl acetate, drying over anhydrous $MgSO_4$, filtration and concentration, the crude product was purified by column chromatography.

2.4.4 Buchwald–Hartwig Amination and Etherification

A flame-dried 50 mL round-bottom flask equipped with a magnetic stirbar and a rubber septum were charged with aryl halide (1.0 mmol), aniline (1.1 mmol) or phenol (1.1 mmol), K_2CO_3 (2.0 mmol) and CL-salen-Pd(II) (1.0% mmol). DMSO (5.0 mL) was then added and the mixture was heated to 80 ℃ for 12 h. The mixture was cooled to room temperature, quenched with water (5 mL), and extracted with 3 × 5 mL of ethyl acetate. The combined organic extracts were dried over anhydrous magnesium sulfate, filtered, and concentrated in vacuo. Finally, the crude product was purified by column chromatography.

2.5 Recyclability Study of the Cellulosic Pd(salen)-Type Catalyst

In this work, cyclic performance of cellulosic Pd(salen)-type catalyst was detected by repeated Suzuki coupling reaction. After filtered and washed thoroughly with water and ethanol, the catalyst was then dried in *vacuo* at 50 ℃ overnight, and reused for subsequent different cross-coupling experiments under similar reaction conditions (Sect. 2.4).

3 Results and Discussion

3.1 Characterization of the Catalyst

Figure 1 shows the FT-IR spectra of CL, CDC, ADC, Cell-Schiff base and CL-salen-Pd(II). The FT-IR spectrum of CDC is shown in Fig. 1b. Compared to CL (Fig. 1a), the new spectral band appears at 700 cm^{-1}, which corresponds to the stretching vibration of C–Cl bond. After modification with ethylenediamine, the new absorption peaks can be obviously

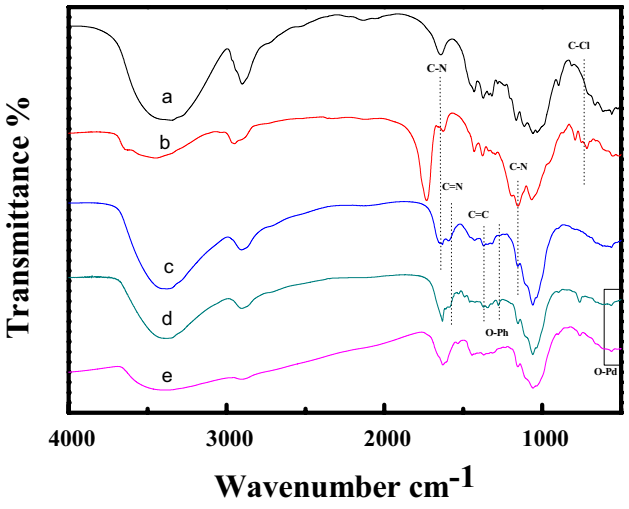

Fig. 1 FT-IR spectra of a CL, b CDC, c ADC, d Cell-Schiff base and e CL-salen-Pd(II)

observed at 1650 1170 and 1055 cm^{-1} in the FT-IR spectrum of ADC (Fig. 1c), which are attributed to the stretching vibration of primary amine ($V_{C–N} + V_{N–H}$) and secondary amine ($V_{C–N} + V_{N–H}$), respectively. The FT-IR spectrum of Schiff base-modified cellulose is shown in Fig. 1d. the pecks at about 1525 and 1255 cm^{-1} assign to the stretching vibration of the benzenoid C = C and O benzene ring which come from Schiff base structure. Besides, the stretching vibration of C = N bond was observed at 1625 cm^{-1}, indicating that salicylaldehyde reacted successfully with ADC to form the corresponding Schiff base structure. After the coordination of Cell-Schiff base ligand to palladium chloride (Fig. 1e), the new stretching vibration at 515–600 cm^{-1} are due to coordination bond which formed by the palladium ions and N atom. This result was consistent with previous literature reports [51, 52], which proves that our catalytic system has been constructed successfully.

The surface morphological studies were then carried out by scanning electron microscopy (SEM). The SEM images of CL, CDC, ADC, Cell-Schiff base and CL-salen-Pd(II) are shown in Fig. 2. The morphological structure of microcrystalline cellulose (starting material) has non-nanofibre and non-pore characteristics (Fig. 2a). The SEM image of CDC revealed that some cross-linked nanofibre were obtained after dealing with thionyl chloride (Fig. 2b). The SEM of ADC shows higher agglomeration degree compared to CDC (Fig. 2c), may be caused by the cross-linking of nanofibers with the addition of ethylenediamine. The SEM image of Cell-Schiff base displays a foamy porous structure (Fig. 2d), which is more beneficial to the coordination between the ligand-anchored cellulose and palladium species. According to the SEM image of CL-salen-Pd(II) (Fig. 2e), it can be observed similar porous structure to the Cell-Schiff base on

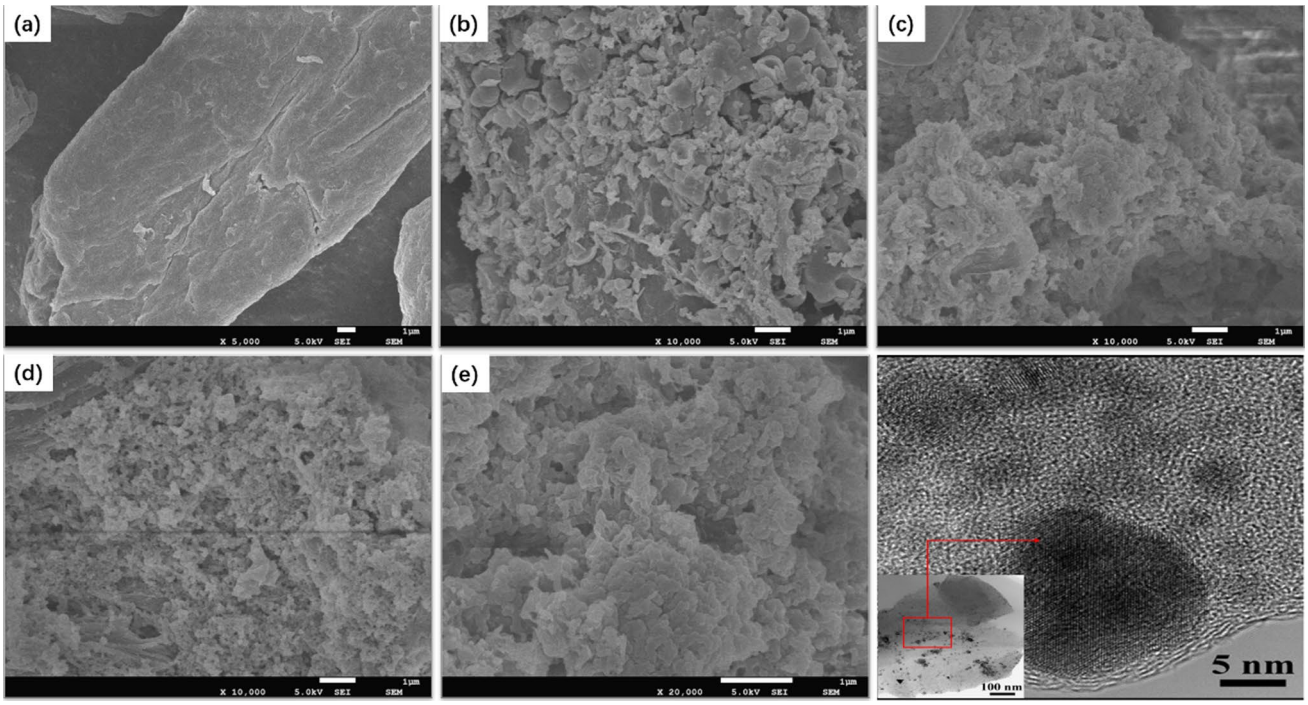

Fig. 2 SEM images of **a** CL, **b** CDC, **c** ADC, **d** Cell-Schiff base, **e** CL-salen-Pd(II) and **f** TEM images of CL-salen-Pd(II)

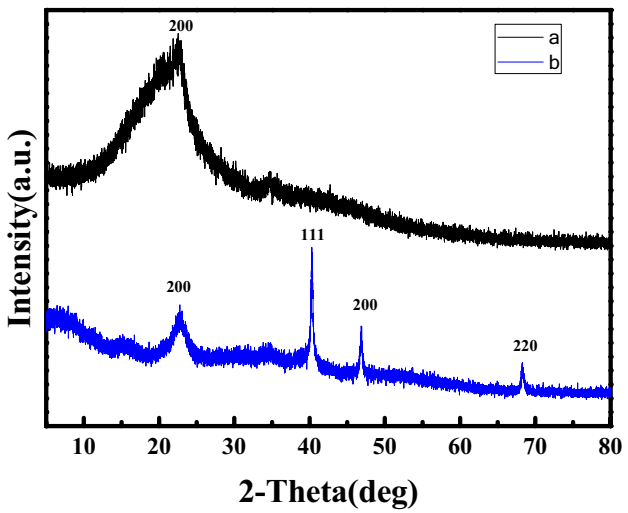

Fig. 3 XRD patterns of a Cell-Schiff base and b CL-salen-Pd(II)

our catalyst. The slightly cross-linked structure demonstrates the successful formation of the cellulosic Pd(salen)-type catalytic complex. From the TEM image of the CL-salen-Pd(II) (Fig. 2f), it is obvious that the palladium is uniformly distributed on the surface of the catalyst, and its particle size is uniform, ranging from 5 to 10 nm.

The crystal structure of Cell-Schiff base and the cellulosic Pd(salen)-type catalyst were investigated using XRD (Fig. 3). The wide diffraction peak at $2\theta = 22.5°$ is referred to the (200) diffraction planes of cellulose [53]. From Fig. 3b we still can clearly find that this peak remains in its position, but the strength is reduced, indicating that palladium coordination would not destroy the basic structure of cellulose during catalyst preparation. In addition, the index peaks at $2\theta = 40.1°$, 46.6° and 68.2° correspond to diffractions from various lattice planes of (111), (200) and (220) present in the cubic palladium [54], confirming the presence of palladium on the cellulose.

The XPS spectrum of cellulosic Pd(salen)-type catalyst was carried out to further understand the surface composition and the state of Pd crystal (Fig. 4). The binding energies of the doublet peaks locate at Pd $3d_{5/2}$ (337.1 eV) and Pd $3d_{3/2}$ (342.4 eV) respectively, which can be attributed to the Pd(II) state [55]. These results indicated that the Pd species on Cell-Schiff base was of the Pd(II) state and no Pd(0) state existed in this cellulosic Pd(salen)-type catalytic complex. The inset image shows the survey spectrum of the cellulosic Pd(salen)-type catalytic complex. The signal of Pd was weaker than those of elements C, N and O because Cell-Schiff base was not fully covered by Pd NPs. Besides, this new ligand anchored cellulose chelated near 1.725 mol kg^{-1} of palladium, as determined by ICP-AES analysis.

The thermal stability of supported catalyst has a great influence on the activity and reusability of the catalyst. Therefore, the thermal stability of CL, Cell-Schiff base and CL-salen-Pd(II) were investigated by Thermal Gravity Analysis. As illustrated in Fig. 5a, the decomposition temperature

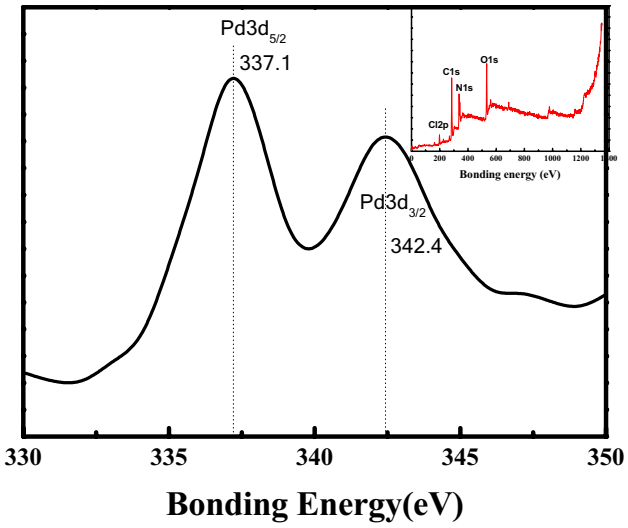

Fig. 4 XPS spectrum of the cellulosic Pd(salen)-type catalytic complex

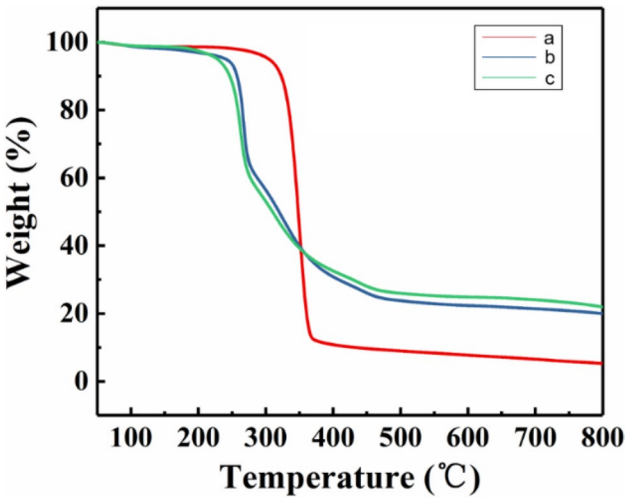

Fig. 5 TG curves of a CL, b Cell-Schiff base and c CL-salen-Pd(II)

of CL is at 320 ℃. Nevertheless, the weight loss of the Cell-Schiff base (Fig. 5b) starts at around 255 ℃, demonstrating cellulose is successfully modified. Finally, according to the TG curve of CL-salen-Pd(II) (Fig. 5c), it could be observed that the initial weight loss of the catalyst is near to 100 ℃ (3.5%), which may be due to the weight loss of water trapped on its surface. After that The TG curve of the catalyst slowly decreased from 255 ℃, which corresponds to the Schiff base curve. The above results indicate that this cellulosic Pd(salen)-type catalyst has good thermal stability from room temperature to 255 ℃. It can be concluded that our catalyst is an effective catalyst to carry out different cross-coupling reactions at 80 ℃ without any decomposition under experimental conditions.

3.2 Catalytic Activity of the Cellulosic Pd(salen)-Type Catalyst for Different Cross-Couplings

To evaluate the catalytic performance of cellulosic Pd(salen)-type catalyst, Suzuki, Heck, and Sonogashira carbon–carbon cross-coupling reactions were chosen as model reactions, and the results are summarized in Tables 1, 2, and 3. At first, it was used in Suzuki cross-couplings (Table 1). In general, this catalyst is efficient for the synthesis of biaryl products **3** in high to excellent yields. The nature of aryl halides was very important to the reaction outcome. Both aryl bromides and iodides displayed excellent reactivity, however, the use of aryl chlorides afforded inferior results than their iodo or bromo analogues (**3aa**, Table 1). No desired product was obtained, probably attributed to poorer tendency of C–Cl bond to undergo oxidative addition by the CL-salen-Pd(II) in mild reaction conditions. Arylboric acids with both electron-donating (–OMe) and electron-withdrawing (–CF_3, –Cl) groups can smoothly undergo the Suzuki cross-coupling reaction, moreover, heterocyclic boronic acid (2-thiopheneboronic acid) was also suitable substrate to afford the corresponding product in 85% yield. When 1,4-dibromobenzene was used as a substrate, terphenyl product can be obtained in 94%. It is worth noting that an aqueous Suzuki cross-coupling was examined in the presence of this cellulosic Pd(salen)-type catalyst, biphenyl product **3aa** can be isolated in 97% yield.

The activity of this catalyst was then investigated in Heck cross-couplings (Table 2). Similar to Suzuki cross-coupling process, aryl iodides and bromides were suitable substrates, and excellent yields were obtained for all the cases. The mild reaction conditions were compatible with various functionalities including methoxy, chlorine, and ester. Electron-rich and electron-deficient groups of aryl halides displayed similar results in yields. No ester hydrolysis was observed when alkene coupling partners had ester residues.

The Sonogashira coupling reactions of various aryl iodides and aryl bromides with terminal alkynes were finally explored using this cellulosic Pd(salen)-type catalyst (Table 3). Different from the above Suzuki and Heck reactions, aryl chloride was also applicable, giving 7aa in 96% yield. For aryl iodides, the coupling reaction proceeded smoothly and provided the corresponding products in good to excellent yields. For aromatic terminal alkynes, electron withdrawing or donating substituents (Br, CN and OMe) were tolerated, affording products **7ab**–**7ad** in 93–95% yields. Hetero-aromatic 2-ethynylpyridine can also undergo well to give **7ae** in 78% yield. Finally, both aliphatic terminal alkyne and ester propiolate were suitable substrates to provide the corresponding products in 83% and 87%, respectively.

Table 1 Suzuki cross-coupling reaction of aryl halides and arylboronic acids

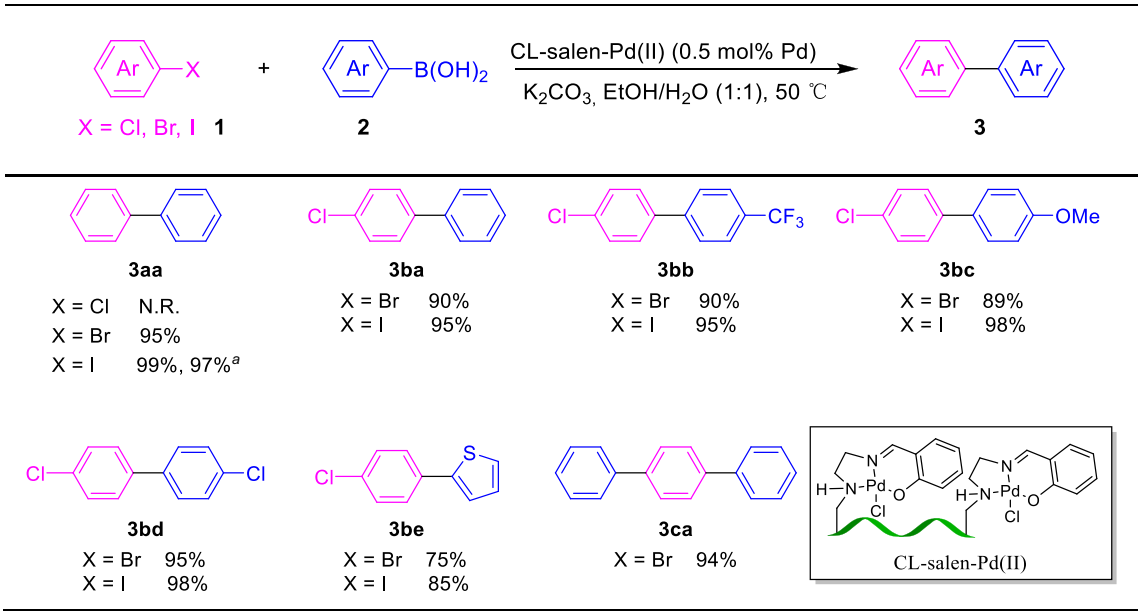

Reaction conditions: 1.0 mmol aryl halide, 1.1 mmol arylboronic acid, 11.1 mg of CL-salen-Pd(II) (0.5 mol %), 2.0 mmol K_2CO_3, 5.0 mL solvent, 50 ℃, 1 h

Isolated yields

[a]Water was used as the solvent

Table 2 Heck reaction of aryl halides with alkenes

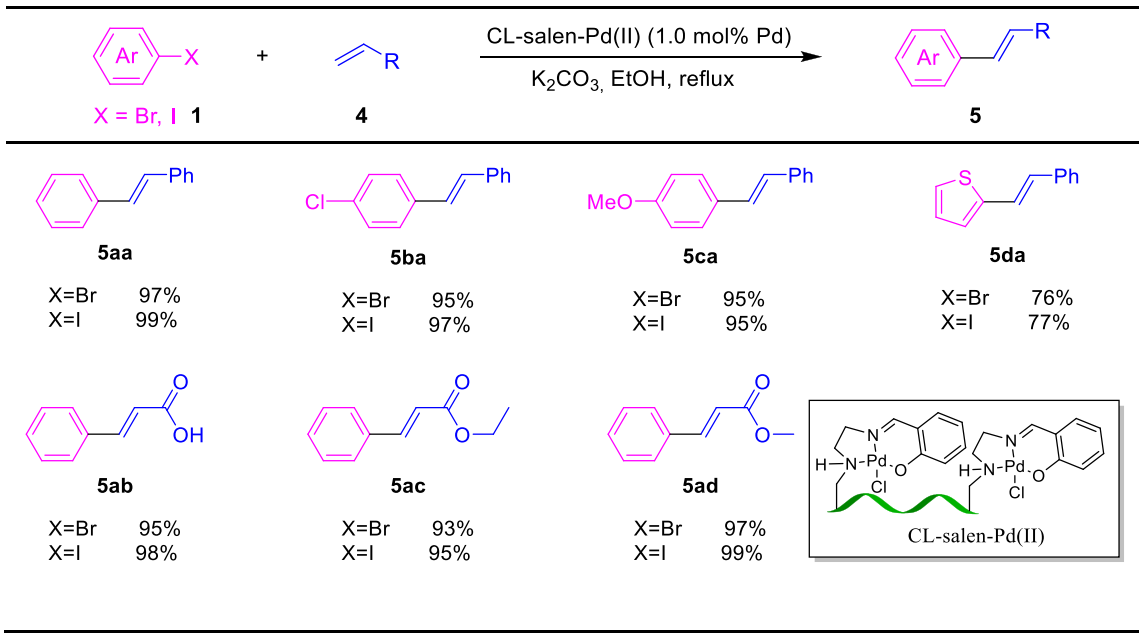

Reaction conditions: 1.0 mmol aryl halide, 1.1 mmol alkene, 22.3 mg of CL-salen-Pd(II) (1.0 mol % Pd), 2.0 mmol K_2CO_3, 5.0 mL ethanol, reflux, 3 h

Isolated yields

The catalytic activity of the cellulosic Pd(salen)-type catalyst was further investigated for carbon-heteroatom bond formation, such as Buchwald–Hartwig amination and etherification reaction (Fig. 6). Iodobenzene **1a** was utilized to react with phenol and aniline at 80 ℃ in DMSO, diphenyl ether **9aa** and diphenyl amine **9ab** can be isolated in 93%

Table 3 Sonogashira cross-coupling reaction of aryl halides with terminal alkynes

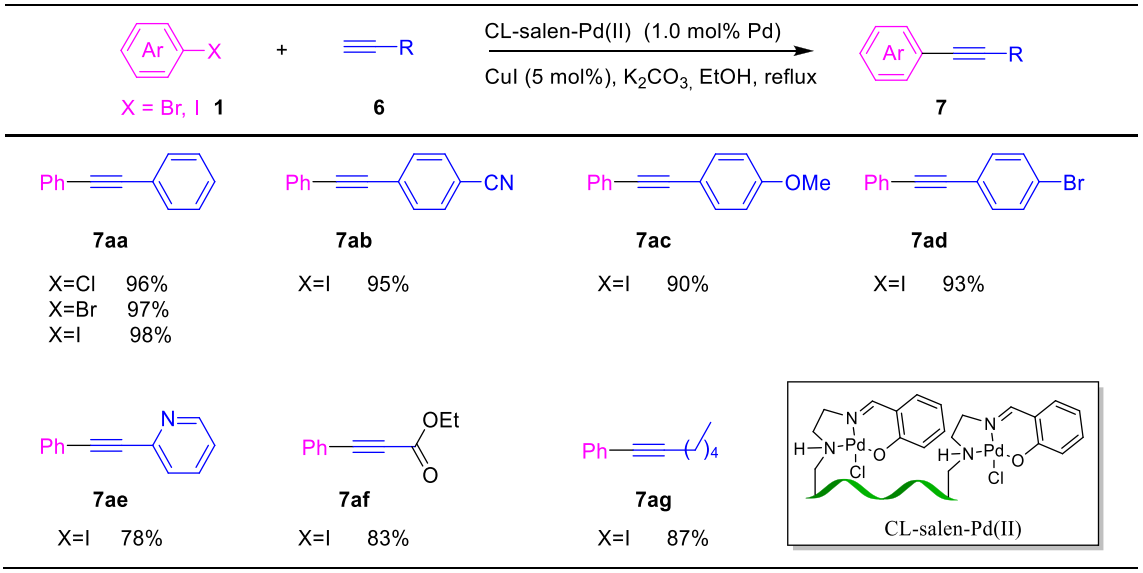

Reaction conditions: 1.0 mmol aryl halide, 1.1 mmol terminal alkyne, 22.3 mg of CL-salen-Pd(II) (1.0 mol% Pd), 0.05 mmol CuI, 2.0 mmol K_2CO_3, 5.0 mL ethanol, reflux, 3 h

Isolated yields

Fig. 6 CL-salen-Pd(II) catalyzed Buchwald–Hartwig amination and etherification

and 78% yields respectively. The above results demonstrated our catalyst was versatile toward all types of cross-coupling reactions.

The compared results achieved in the work with other biopolymer-based catalysts for the Suzuki, Heck, Sonogashira Buchwald–Hartwig amination and etherification coupling reactions, which are summarized in Table 4. In comparison with other catalysts in Suzuki reaction, it is clear that each method has its own advantages. However, our work has some merits, such as lower reaction temperatures, high yields and without using any other instruments like microwave ovens (Table 4, entries 1–6). As for the Heck reaction, taking iodobenzene reacting with styrene as an example, the results are listed in Table 4, entries 7–12. These data show that our catalyst is more efficient than other catalysts, producing high reaction yields with obviously lower reaction temperature and utilization of green solvent. To compare the efficiency of our catalyst with those of other catalysts reported for the Sonogashira reaction, we chose the reaction between iodobenzene and phenylacetylene. As shown in Table 4, entries 13–18, our catalyst showed some extensive improvement in reaction conditions, such as reaction temperature, solvent and yield. It is worth noting that when comparing the synthesized sample with CNC-BIA-Pd catalyst (Table 4, entries 19–20), it can be observed the fact that the catalyst activity still needs to be improved in the Buchwald–Hartwig etherification reaction. Interestingly, we report the first example of cellulose-supported Pd catalysts as efficient and sustainable catalyst systems for Buchwald–Hartwig amination reactions. Finally, it can be concluded that the catalyst is a desirable alternative because it not only shows particularly good activity in traditional carbon–carbon coupling but also plays an important role in the formation of carbon-hetero bonds.

3.3 Recyclability Study of the Cellulosic Pd(salen)-Type Catalyst

To check the heterogeneity of catalyst, a hot filtration test on the cellulosic Pd(salen)-type catalyst using the model

Table 4 Catalytic performance of different Pd-based catalysts in coupling reactions

Entry	Catalyst	Condition	Yield (%)	References
1[a]	Cell-Pd(0)	K_2CO_3/H_2O,100℃	83	[56]
2[a]	Cell-$OPPh_3$-Pd(0)	K_2CO_3/EtOH, 80℃	95	[44]
3[a]	CL-Sc-Pd(II)	K_2CO_3/Solvent-free, MW	99	[49]
4[a]	CL-DETA-Pd	K_2CO_3/EtOH: H_2O (1:1),75℃	96	[51]
5[a]	Cell-Sb-Pd(II)	K_2CO_3/EtOH: H_2O (1:1),70℃	99	[57]
6[a]	CL-salen-Pd(II)	K_2CO_3/EtOH: H_2O (1:1),50℃	99	This work
7[b]	Cell-Pd(0)	Et_3N/CH_3CN, 120℃	100	[41]
8[b]	Cell-$OPPh_2$-Pd(0)	Bu_3N/DMF, 110℃	91	[43]
9[b]	PdNPs@CNCs	K_2CO_3/CH_3CN: H_2O (1:1),100℃	75	[58]
10[b]	CMC-Pd^{II}	$K_3PO_4{\cdot}3H_2O$/DMF, 110℃	85	[59]
11[b]	PdNP@CNXL	NaOAc/CH_3CN: H_2O (1:1),100℃	87	[60]
12[b]	CL-salen-Pd(II)	K_2CO_3/EtOH, Reflux	99	This work
13[c]	Cell-Pd(0)	Et_3N/CH_3CN, Reflux	98	[41]
14[c]	Cell-O_2PPh_3-Pd(0)	Et_3N/DMF, 80℃	95	[45]
15[c]	PdNPs@XH	Et_3N/CH_3CN, 90℃	96	[61]
16[c]	Pd-MNPSS	K_2CO_3/H_2O, 100℃	87	[62]
17[c]	Pd/Cu@MMT/CS	PPh_3,Na_2CO_3/DME: H_2O (4:1) 80℃	96	[63]
18[c]	Cell-half-salen-Pd(II)	K_2CO_3/EtOH, Reflux	98	This work
19[d]	CNC-BIA-Pd	K_2CO_3/DMSO, 80℃	96	[64]
20[d]	CL-salen-Pd(II)	K_2CO_3/DMSO, 80℃	93	This work
21[e]	CL-salen-Pd(II)	K_2CO_3/DMSO, 80℃	78	This work

[a]Suzuki coupling reaction

[b]Heck coupling reaction

[c]Sonogashira coupling reaction

[d]Buchwald-Hartwig etherification reaction

[e]Buchwald-Hartwig amination reaction

Suzuki-coupling reaction was performed. After reacting for one hour under optimized reaction conditions, the reaction mixture was filtered under thermal conditions, and then the filtrate was heated under the same reaction conditions. Interestingly, no further reactions were observed at all. Besides, the ICP-AES analysis of the filtrate revealed that no palladium species were leached out into the aqueous solution. Therefore, the results verify that the catalytic process is heterogeneous catalysis.

The recyclability of the cellulosic Pd(salen)-type catalyst was investigated by repetitive experiment on the model Suzuki–Miyaura cross-coupling reaction. (Fig. 7). The CL-salen-Pd(II) was recycled by simple centrifugation, washing with water to remove the salt after reaction completion. The catalytic activity decreased slightly after the second cycle however, the yields of Suzuki cross-coupling reaction can still reach up to 90% after twelve times cycles with a slight loss of activity. In addition, the palladium content of the reaction materials before and

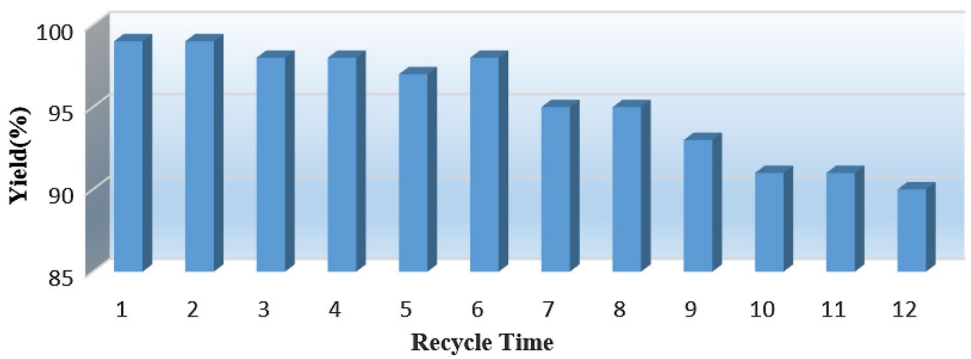

Fig. 7 Recycling test of the CL-salen-Pd(II)

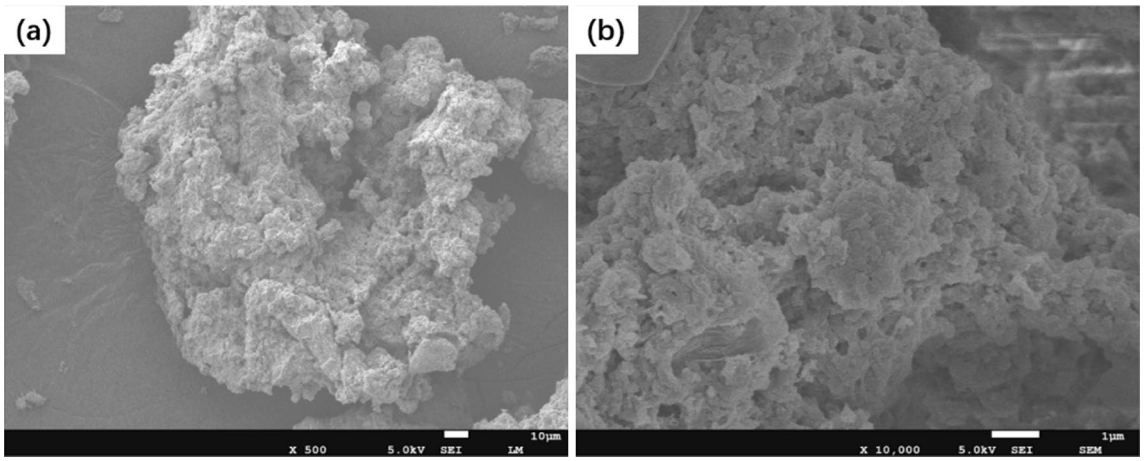

Fig. 8 SEM image of CL-salen-Pd(II) after the 12th runs

after the cycle by ICP-AES was also analyzed. It could be found that the palladium content in the starting reaction mass was 1.73 mol kg^{-1}, and the palladium content was 1.69 mol kg^{-1} after the cycle twelve-times. The result of the palladium leaching ratio of only 2.31% is satisfactory. Additionally, SEM analysis of used CL-salen-Pd(II) was performed to determine any changes in the shape and size of nanoparticles, and it was observed that the surface morphology of catalyst did not change (Fig. 8). Therefore, all above results proved that the ligand-anchored cellulose can be firmly coordinated to palladium center, thus avoiding the leaching of catalytic active species.

4 Conclusion

In conclusion, we have designed, prepared, and characterized cellulosic Pd(salen)-type catalytic complex as a reusable heterogeneous catalyst. This novel and efficient catalyst shows good activity in five different types of cross-coupling reactions (such as Suzuki, Heck, Sonogashira, Buchwald–Hartwig amination and etherification). Excellent yields, mild reaction periods and conditions, high chemical and thermal stability are the important advantages of this catalyst. Furthermore, this catalyst was also easily recycled without obvious loss in the catalytic activity even after twelve times cycles. Further applications are currently explored for other types of reactions in our laboratories.

Funding This work was supported by the Fundamental Research Funds for the Central Universities (2572017DB07) and Natural Science Foundation of Heilongjiang Province (B2017002).

References

1. Seechurn CCCJ, Kitching MO, Colacot TJ, Snieckus V (2012) Angew Chem Int Ed 51:5062–5085
2. Gildner PG, Colacot TJ (2015) Organometallics 34:5497–5508
3. Budagumpi S, Haque RA, Salman AW (2012) Coordin Chem Rev 256:1787–1830
4. Molander GA, Canturk B (2008) Org Lett 10:2135–2138
5. Kobayashi H, Komanoya T, Guha SK, Hara K, Fukuoka A (2011) Appl Catal A 409:13–20
6. Fukuoka A, Dhepe PL (2009) Chem Rec 9:224–235
7. Sarkar SM, Rahman ML, Chong KF, Yusoff MM (2017) J Catal 350:103–110
8. Lim H, Cha MC, Chang JY (2012) Polym Chem 3:868–870
9. Seki M (2006) Synthesis 18:2975–2992
10. Varma RS, Naicker KP, Liesen PJ (1999) Tetrahedron Lett 40:2075–2078
11. Ghotbinejad M, Khosropour AR, Mohammadpoor-Baltork I, Moghadam M, Tangestaninejad S, Mirkhani V (2014) RSC Adv 4:8590–8596
12. Baran T (2019) Catal Lett 149:1496–1503
13. Baran T, Mentes A (2017) J Mol Struct 1134:591–598
14. Veisi H, Najafi S, Hemmati S (2018) Int J Biol Macromol 113:186–194
15. Bao YH, Shao LJ, Xing GY, Qi CZ (2019) Int J Biol Macromol 130:203–212
16. Su YC, Ma LY, Chen J, Xu JH (2017) Carbohyd Polym 175:113–121
17. Hajipour AR, Khorsandi Z, Abeshtian Z (2019) Inorg Chem Commun 107:107470
18. Baran T, Baran NY, Mentes A (2018) Int J Biol Macromol 115:249–256
19. Baran T (2018) Carbohyd Polym 195:45–52
20. Baran T, Baran NY, Mentes A (2018) Appl Organometal Chem 32:e4076
21. Klemm D, Heublein B, Fink HP, Bohn A (2005) Angew Chem Int Ed 44:3358–3393
22. Habibi Y, Lucia LA, Rojas OJ (2010) Chem Rev 110:3479–3500
23. Moon RJ, Martini A, Nairn J, Simonsen J, Youngblood J (2011) Chem Soc Rev 40:3941–3994
24. Kaushik M, Moores A (2016) Green Chem 18:622–637
25. An XY, Long YD, Ni YH (2017) Carbohyd Polym 156:253–258

26. Liang M, Zhang G, Feng YJ, Li RL, Hou P, Zhang JS, Wang JM (2018) J Mater Sci 53:1568–1579
27. Abdulwahab MI, Khamkeaw A, Jongsomjit B, Phisalaphong M (2017) Catal Lett 147:2462–2472
28. Chen MY, Kang HL, Gong YM, Guo J, Zhang H, Liu RG (2015) ACS Appl Mater Inter 7:21717–21726
29. Yan W, Chen C, Wang L, Zhang D, Li AJ, Yao Z, Shi LY (2016) Carbohyd Polym 140:66–73
30. Zhi YF, Deng XF, Ni YH, Zhao WB, Jia QM, Shan SY (2018) Carbohyd Polym 194:170–176
31. Goswami M, Das AM (2018) Carbohyd Polym 195:189–198
32. Pourjavadi A, Habibi Z (2015) RSC Adv 5:99498–99501
33. Baran T (2019) Catal Lett 149:1721–1729
34. Jebali Z, Granados A, Nabili A, Boufi S (2018) do Rego AMB, Majdoub H, Vallribera A. Cellulose 25:6963–6975
35. Yuan FS, Huang Y, Fan MM, Chen CT, Qian JS, Hao QL, Yang JZ, Sun DP (2018) Chem Eur J 24:1844–1852
36. Yasukawa T, Miyamura H, Kobayashi SU (2015) Chem Sci 6:6224–6229
37. Jana R, Pathak TP, Sigman MS (2011) Chem Rev 111:1417–1492
38. Chen QA, Ye ZS, Duan Y, Zhou YG (2013) Chem Soc Rev 42:497–511
39. Beccalli EM, Broggini G, Martinelli M, Sottocornola S (2007) Chem Rev 107:5318–5365
40. Wu WQ, Jiang HF (2012) Acc Chem Res 45:1736–1748
41. Reddy KR, Kumar NS, Reddy PS, Sreedhar B, Kantam ML (2006) J Mol Catal A 252:12–16
42. Mirosanloo A, Zareyee D, Khalilzadeh MA (2018) Appl Organomet Chem 32:e4546
43. Du QW, Li YQ (2012) Res Chem Intermediat 38:1807–1817
44. Wang XX, Xu YJ, Wang F, Wei YP (2015) J Appl Polym Sci 132:41427
45. Lu ZC, Jasinski JB, Handa S, Hammond GB (2018) Org Biomol Chem 16:2748–2752
46. Shirase S, Shinohara K, Tsurugi H, Mashima K (2018) ACS Catal 8:6939–6947
47. Xiong G, Chen XL, You LX, Ren BY, Ding F, Dragutan I, Dragutan V, Sun YG (2018) J Catal 361:116–125
48. Rezaei G, Naghipour A, Fakhrio A (2018) Catal Lett 148:732–744
49. Baran T, Baran NY, Mentes A (2018) J Mol Struct 1160:154–160
50. Baran NY, Baran T, Mentes A (2017) Appl Catal A 531:36–44
51. Dong YH, Lai Y, Wang XX, Gao M, Xue FJ, Chen XF, Ma YS, Wei YP (2019) Int J Biol Macromol 130:778–785
52. Liu LB, Xu Y, Xu MJ, Li B (2019) Compos Part B 167:422–433
53. Peng XW, Ren JL, Zhong LX, Sun RC (2011) Biomacromol 12:3321–3329
54. Son SU, Jang Y, Park J, Na HB, Park HM, Yun HJ, Lee J, Hyeon T (2004) J Am Chem Soc 126:5026–5027
55. Ding SY, Gao J, Wang Q, Zhang Y, Song WG, Su CY, Wang W (2011) J Am Chem Soc 133:19816–19822
56. Jamwal N, Sodhi RK, Gupta P, Paul S (2011) Int J Biol Macromol 49:930–935
57. Dong YH, Bi JJ, Zhu DJ, Meng D, Ming SJ, Guo W, Chen Z, Liu Q, Guo L, Li T (2019) Cellulose 26:7355–7370
58. Cirtiu CM, Dunlop-Briere AF, Moores A (2011) Green Chem 13:288–291
59. Xiao JL, Lu ZX, Li YQ (2015) Ind Eng Chem Res 54:790–797
60. Rezayat M, Blundell RK, Camp JE, Walsh DA, Thielemans W (2014) ACS Sustainable Chem Eng 2:1241–1250
61. Chen W, Zhong LX, Peng XW, Wang K, Chen ZF, Sun RC (2014) Catal Sci Technol 4:1426–1435
62. Tukhani M, Panahi F, Khalafi-Nezhad A (2018) ACS Sustainable Chem Eng 6:1456–1467
63. Liu Q, Xu MD, Zhao J, Yang Z, Qi CZ, Zeng MF, Xia R, Cao XZ, Wang BY (2018) Int J Biol Macromol 113:1308–1315
64. Seyednejhad S, Khalilzadeh MA, Zareyee D, Sadeghifar H, Venditti R (2019) Cellulose 26:5015–5031

Affiliations

Peng Sun[1,2] · Jiaojiao Yang[1] · Chunxia Chen[1,2] · Kaijun Xie[1] · Jinsong Peng[1]

✉ Chunxia Chen
ccx0109@nefu.edu.cn

✉ Jinsong Peng
jspeng1998@nefu.edu.cn

[1] College of Chemistry, Chemical Engineering and Resource Utilization, Northeast Forestry University, Harbin 150040, Heilongjiang, People's Republic of China

[2] Material Science and Engineering College, Northeast Forestry University, Harbin 150040, Heilongjiang, People's Republic of China